Mechanical Property Modification and Morphology of Poly(styrene-*b*-hydrogenated butadiene-*b*-styrene)/ Poly(hydrogenated butadiene) Blends

J. P. Baetzold, I. Gancarz,[1] X. Quan,[2] and J. T. Koberstein*,[3]

Department of Chemical Engineering and Institute of Materials Science, University of Connecticut, Storrs, Connecticut 06269-3136

Received October 26, 1993; Revised Manuscript Received June 20, 1994®

ABSTRACT: The mechanical properties and morphology of a series of triblock copolymer blends with midblock associating homopolymers of varing molecular weights have been characterized. The symmetric triblock copolymer studied contains polystyrene endblocks and midblocks of hydrogenated poly(1,2-butadiene) and is mixed with hydrogenated poly(1,2-butadiene) homopolymers of molecular weights both below and above that of the copolymer midblock. The rubbery plateau modulus determined by dynamic mechanical spectroscopy increases with increasing molecular weight of the homopolymer at fixed overall homopolymer content. At fixed molecular weight, the composition dependence of the plateau modulus is complex and shows unusually synergistic behavior. For high molecular weight homopolymers (i.e., with molecular weights equal to or exceeding that of the midblock), the plateau modulus increases initially upon homopolymer addition, in contrast to what is expected to occur when an additional rubbery component is added to an elastomer. Small angle neutron scattering and transmission electron microscopy are employed to determine the morphological changes induced by homopolymer addition. In all cases, the blends exhibit a lamellar microphase structure, with homopolymer macrophases apparent at high homopolymer contents. The apparent homopolymer solubility limits are found to be inversely related to the homopolymer molecular weight. Microdomain dimensions are determined by model correlation function analysis and by analysis of the interface distribution function. The results indicate that the lamellar repeat distance decreases upon addition of the lowest molecular weight homopolymer and that the microdomains swell in blends containing homopolymers with molecular weights similar to that of the midblock sequence and are unchanged for high molecular weight homopolymers with negligible solubility. The microdomain morphologies of these blends appear to be locally heterogeneous, ruling out the possibility of constructing quantitative structure–property relations. Qualitative molecular models are proposed in order to provide initial explanations for the unusual synergistic properties observed in the blends. The results suggest that the interesting mechanical response of the blends can be explained by consideration of the changes in their entanglement structure resulting from confinement of the homopolymer chains within the highly constrained environment of the midblock lamellae.

Introduction

Block copolymers are important materials due to their extensive technological applicability and as a result of their employment as model systems for the investigation of the structure and thermodynamics of multiconstituent polymers. Early applications of block copolymers were based upon the elastomeric properties that result when a glassy component is linked to a second, incompatible component which is rubbery at the use temperature. Such a material exhibits thermoplastic behavior and can be readily processed by heating above the glass transition temperature of the glassy component.

More recently, a number of specialty applications have arisen for block copolymers in mixtures with, or as additives to, other materials. For example, certain block copolymers have been used as emulsifiers for incompatible homopolymers,[4] as compatibilizers and adhesion promoters for immiscible homopolymer blends,[5] as viscosity modifiers in lubricants,[6] and as mechanical strength modifiers in composites.[7-9] Alternatively, the inclusion of additives within a block copolymer can also be employed to modify the properties of the parent resin, as in the case of tackifiers for adhesive applications of block copolymers.[10] The basic principles regarding the phase diagrams and morphology of mixtures containing block copolymers have been evidenced in various theories and experimental reports. The diverse and complex structures observed offer great promise for novel applications and perhaps synergistic behavior.

Our laboratory has been particularly interested in block copolymers composed from blocks of polystyrene, as the glassy constituent, and either butadiene, isoprene, or their hydrogenated analogs, as the rubbery constituent. Many commercially available resins contain copolymers based on these constituents as major components. Previous work has addressed the microphase separation transition of these copolymers,[11] the effect of homopolymer addition on the microphase separation transition,[12] the chain dimensions of neat block copolymers and their blends,[13] and the efficiency of block copolymers in compatibilizing (i.e. decreasing the interfacial tension of immiscible mixtures of) the two parent homopolymers.[5] The morphology of these blends was generally found to differ from that of the neat copolymer, that is, to change in accordance with the volume of homopolymer added to the system.

The focus of this paper is the influence of homopolymer addition on the mechanical properties and morphology of a polydiene/polystyrene triblock copolymer and follows an initial report[14] on this subject. Early sources of block copolymer blends with homopolymers demonstrated that small amounts of homopolymers could be incorporated within the block copolymer microdomain structure, as long as the molecular weight of the homopolymer was below that of the corresponding copolymer block.[15-20]

The phase diagrams of diblock copolymer/homopolymer blends have been characterized by Roe and Zin.[21] They found that the homopolymer was incorporated (i.e. dissolved) within the microdomain structure of the block copolymer up to a critical concentration, beyond which the homopolymer formed separate macrophases. Similar

* Abstract published in *Advance ACS Abstracts*, August 1, 1994.

0024-9297/94/2227-5329$04.50/0

Table 1. Material Properties

sample designation	sample type	GPC[a] M_n	M_w/M_n after hydrogenation	M_w/M_n before hydrogenation	wt % 1,2 addition	wt % styrene
hCP	poly(styrene-*b*-hydrogenated butadiene-*b*-styrene) triblock copolymer	112K	1.32	1.15	91	49
hB-10	hydrogenated polybutadiene homopolymer	11K	1.14	1.05	95	
hB-30	hydrogenated polybutadiene homopolymer	32K 24[b]	1.07	1.07	95	
hB-60	hydrogenated polybutadiene homopolymer	58K	1.09	1.03	93	
hB-120	hydrogenated polybutadiene homopolymer	138 122[b] 146[b]	1.13	1.03	98	

[a] PS calibration. [b] Membrane osmometry.

solubility behavior has been predicted[22] for mixtures for a diblock copolymer with one of its parent homopolymers. Moreover, a change in microphase geometry is predicted upon homopolymer addition (e.g. from lamellar to cylindrical) as the relative volume fraction of the two species is altered. A recent experimental investigation[23] demonstrated that the morphology of diblock copolymer/homopolymer systems is a function of the homopolymer molecular weight and concentration, block copolymer composition and molecular weight, and the interaction parameter.

The mechanical and rheological properties of block copolymer/homopolymer blends have also been reported.[7,10,24] Han et al.[24] carried out rheological investigations of the order–disorder transitions and dynamic viscoelastic properties in blends of a poly(styrene-*b*-isoprene-*b*-styrene) triblock copolymer with endblock-associating resins. They observed an increase in the rubbery plateau modulus upon resin addition. This increase was attributed to association of the resin with the endblock and the subsequent increase in volume fraction of the glassy microphase. They also found that the glass transition temperature of the rubbery phase increased upon resin addition and concluded that some of the resin must reside within the rubbery midblock domain. In a similar study, Kim et al.[10] showed that adding a midblock-associating resin to a poly(styrene-*b*-isoprene-*b*-styrene) triblock copolymer decreased the rubbery plateau modulus and increased the glass transition temperature of the rubbery midblock. The order–disorder transition temperature was found to decrease as the amount of midblock-associating resin was increased.

In this paper we investigate the solubility behavior of midblock-associating homopolymers added to a poly(styrene-*b*-(hydrogenated 1,2-butadiene)-*b*-styrene) triblock copolymer and the associated effects on the microdomain morphology and mechanical properties. A related paper addresses the spatial distribution of homopolymer molecules dissolved within the block copolymer microdomains.[25]

Experimental Section

The rubbery homopolymer and elastomeric sequence of the block copolymer studied were based upon 1,2-butadiene precursors which were subsequently saturated by hydrogenation. Hydrogenated 1,2-butadienes were chosen because of their resistance to thermal and UV degradation, their high scattering contrast density with respect to styrene for small angle neutron scattering experiments, and the ability to control the amount of contrast by selective deuteration.

The polybutadiene precursor homopolymers were prepared by anionic polymerization in benzene solvent at room temperature under high purity argon gas. *n*-Butyllithium (*n*-BuLi) was used as the initiator and 1,2-dipiperidinoethane was used to obtain a microstructure with greater than 95% 1,2-isomer.[26] The benzene was dried over calcium hydride and distilled from a sodium–benzophenone complex. The monomer was dried over calcium hydride and distilled from *n*-BuLi or a *n*-butylmagnesium. The poly(styrene-*b*-butadiene-*b*-styrene) precursor was synthesized by sequential anionic polymerization, using a similar procedure with a monofunctional initiator.[27]

The butadiene microstructure of the precursor homopolymers and triblock copolymer, the percent styrene present in the triblock copolymer, and the extent of the hydrogenation reaction were determined from proton NMR data. Proton NMR spectra were collected on solutions of the materials in $CDCl_3$ using 90 MHz JEOL, 80 MHz Bruker, and 250 MHz Bruker instruments. The aromatic peaks at 7–8 ppm were used to calculate the amount of styrene in the triblock copolymer. The vinyl peaks at 5–6 ppm were used to determine the microstructure of the butadiene sequences, and the extent of the hydrogenation was monitored by the disappearance of the vinyl peaks at 5–6 ppm. All data were referenced to the spectrum of TMS.

Saturation was carried out using a homogeneous catalyst[28–30] consisting of a complex of *n*-BuLi and the cobalt salt of 2-ethylhexanoic acid in cyclohexane. In order to obtain complete conversion, a mole ratio of 2.5 Li/Co was used. A 1–2 wt % polymer solution with small amounts of *n*-BuLi was injected under vacuum into a 400 mL stainless steel Parr bomb. The bomb was filled with 5–7.5 mol % of catalyst, heated to 50 °C, pressurized to 50–60 psi reactant gas pressure, and stirred for 1–4 h. The reactant gas was either hydrogen, deuterium, or a mixture of both in order to control the neutron scattering cross section of each polymer[13] (also see SANS results in the upcoming paper[25]). For partially deuterated species, the catalyst solution was transferred with deuterium into the bomb which was then pressurized to 50 psi with deuterium, and further pressurized to 60 psi with hydrogen.

Infrared analysis (Digilab FTS-50 FTIR and a Pye-Unicam 3–300 IR spectrometer) for the copolymers was performed on samples with a protonated, deuterated, and partially deuterated midblock. The extent of deuteration was evaluated by analysis of the ratio of the peak areas due to the C—D stretch at 2168 cm^{-1} and the polystyrene band at 1600 cm^{-1} due to ring stretching vibrations.

The characterization results are presented in Table 1. The hydrogenated block copolymer is referred to as hCP, and the hydrogenated polybutadiene homopolymer is hB-*X*, where the *X* refers to the number average molecular weight.

The molecular weights and polydispersities were characterized using a Waters GPC-II and four Waters columns (500, 1000, 10^5, and 10^6 μm) and two Polymer Labs) columns. The carrier solvent was unstabilized THF in the Waters apparatus and toluene for the Polymer Labs system. In each case, the carrier solvent was filtered and degassed before use. Calibration was performed with commercial polystrene standards (Polymer Labs) and the butadiene homopolymers. The number average molecular weights of the copolymer and several butadiene homopolymers were determined from membrane osmometry measurements in toluene solutions with a Knauer membrane osmometer. It was found that the calibration curves for styrene, hydrogenated polybutadiene, and their copolymers were virtually identical when THF was used. This calibration curve was used to determine the molecular weights of hydrogenated block copolymer and

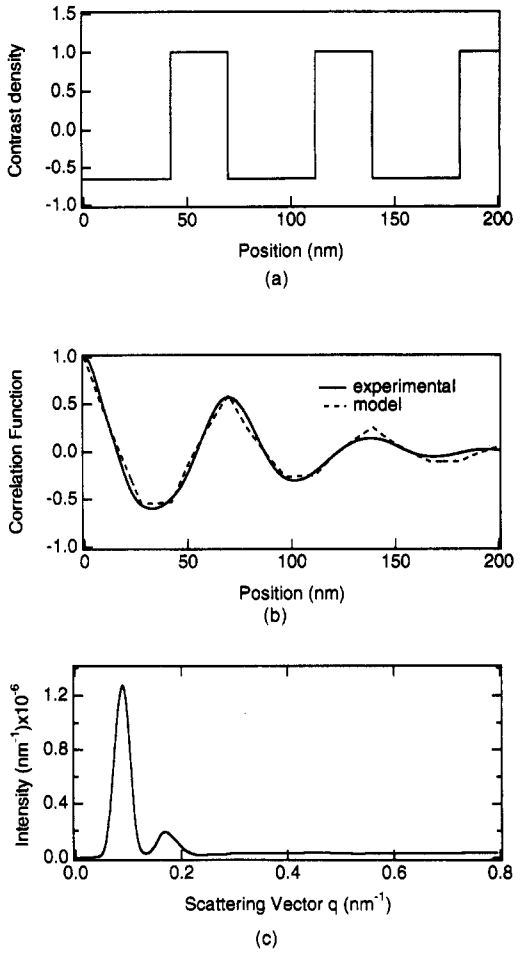

Figure 1. Relationship between (a) the one-dimensional neutron scattering length density profile, (b) the spatial correlation function, and (c) the scattering profile.

hydrogenated homopolymer. The block copolymer was found to contain a small amount of styrene homopolymer (<5%). There was no evidence for the existence of an appreciable diblock fraction.

The hydrogenation reaction broadens slightly the molecular weight distribution over the parent homopolymer. This broadening is expected to have little effect on the morphology of the blends because all materials are unimodal and have relatively narrow distributions. The deuterium and hydrogen saturated analogs therefore have essentially identical molecular lengths and length distributions, but varying neutron scattering contrasts.

Binary blends of the triblock copolymer and homopolymers of varying molecular weight were prepared by solution mixing the components in methylene chloride and casting in machined PTFE molds. Methylene chloride is a good solvent for both constituents but is somewhat preferential toward polystyrene which is the minor component of the blend. Film casting required 2–4 days, after which the samples were placed under vacuum for 1 day. The specimens were subsequently annealed in the molds at 130 °C for 3–5 h under vacuum.

After removal from the molds, the 4–6 mil thick specimens were die-cut into strips 6.3 mm wide for dynamic mechanical analysis using a Rheometrics RDS-2 system. The storage modulus, E', and loss modulus, E'', of the blends were determined over the temperature range −60 to +100 °C at a frequency of 1 rad/s.

Morphology Characterization. Specimens for transmission electron microscopy were cryogenically microtomed at −30 °C using a Sorvall MT 6000 Ultramicrotome with an FS 1000 cryostat. Freshly cut glass knives provided sections that range from 100 to 200 nm in thickness, as estimated by the interference colors. The unstained sections were collected dry onto 400 mesh copper grids and imaged with Phillips 400 and JEOL 100C microscopes with accelerating voltages of 40–80 kV. A slight underfocus was employed to optimize contrast following the methodology reported by Handlin and Thomas.[31]

Specimens for small angle neutron scattering were prepared by slow solvent casting onto matte aluminum substrates, followed by vacuum annealing to remove residual solvent. Most of the SANS experiments were conducted at the 30 m SANS facility at the National Center for Small-Angle Scattering Research at the Oak Ridge National Laboratory. This facility is described in more detail elsewhere.[32] The sample-to-detector distances, source slit, and various pinhole geometries which were used as described in ref 13. Data were acquired on a 64 × 64 cm^2 two-dimensional detector at room temperature using a neutron wavelength of 4.75 Å. The data were corrected for parasitic scattering and sensitivity differences between the cells of the detector and radially averaged. Calibrated standards of porous Al and blends of proteo- and deuterio-polystyrene were used to calibrate the scattered intensity.

Samples were also run on the 10 m SANS facility located at NCSASR. This device employs pinhole geometry, with a sample-to-detector distance and source-to-sample distance of 4.5 m. The source and sample slit diameters were 2.0 and 0.9 cm, respectively. Slit, detector, and wavelength smearing effects were negligible for the geometries employed.

Small Angle Neutron Scattering Analysis. Quantitative analysis of the blend microstructures is accomplished through SANS experiments and subsequent correlation function analysis. The magnitude and sign of the spatial correlation function are related to the probability of finding spatial correlation between similar structural elements. This relationship is depicted schematically in Figure 1 for a system consisting of lamellar stacks oriented randomly on a global scale. Within a particular bundle, the neutron scattering length density, $\beta(z)$ (i.e., the contrast), varies periodically, as depicted in Figure 1a. These fluctuations in density give rise to an angle-dependent scattering intensity, $I(q)$ (Figure 1c) where $q = (4\pi/\lambda)\sin(\theta/2)$, λ is the wavelength and θ is the scattering angle.

The function that relates the density profile to the scattered intensity profile is the spatial correlation function. The correlation function is defined as the autoconvolution of the fluctuation profile, $\eta(z)$, which for a one-dimensional lamellar structure can be written

$$\gamma_{1D}(z) \equiv \int_0^\infty \eta(\xi - z)\eta(\xi)\, d\xi \tag{1}$$

where $\eta(z) \equiv \beta(z) - \langle\beta\rangle$ is the fluctuation in contrast density at position z, and $\langle\beta\rangle$ is the material average contrast density. Analysis of the correlation function can therefore provide information regarding the spatial distribution and sizes of microphases within a material.

The scattered intensity is given by the Fourier transform of the spatial correlation function, which for a one-dimensional lamellar structure is

$$I(q) = K\bar{\eta}^2 \int_0^\infty \gamma_{1D}(z)\cos(qz)\, dz \tag{2}$$

where K is a known constant. From (2) it is evident that an experimental correlation function may be obtained by an inverse Fourier transform according to

$$\gamma_{1D,EXPTL}(z) = \frac{1}{2\pi}\int_0^\infty I(q)q^2\cos(qz)\, dq \tag{3}$$

There are generally two independent approaches for analysis of the correlation function: those based upon constructing a model contrast profile,[33,34] as depicted in Figure 1a, and those based upon statistical treatment of the spatial correlations.[35,36] Statistical methods for direct analysis of the correlation function are difficult to apply for two-phase systems with volume fractions in the range 0.35–0.65 because here the correlation function undergoes only small changes.[37] The present work employs a direct modeling approach involving construction of model contrast density profiles to produce a theoretical correlation function according to (1) and a second statistical method that involves calculation of the interface distribution function.[38]

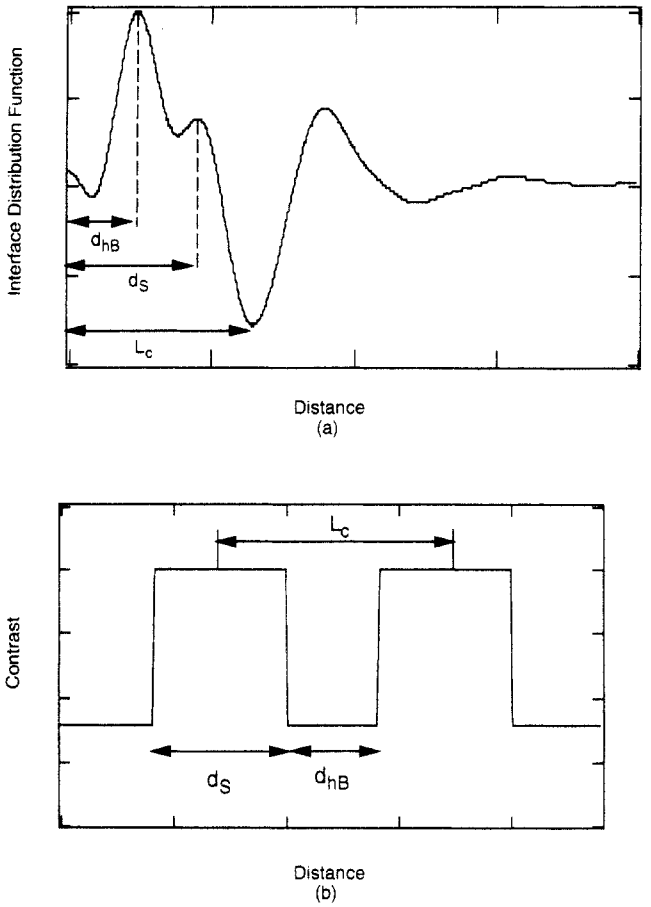

Figure 2. Interface distribution function and its relationship to the contrast density profile. L_c is the correlation length, d_S is the polystyrene microphase thickness, and d_{hB} is the hydrogenated polybutadiene microphase thickness.

The interface distribution function, $g_1(z)$, is determined directly by a cosine Fourier transform of the experimental scattering profile

$$g_1(z) = 8\pi^2 \int_0^\infty \left(\frac{k_1}{2\pi d_p} - s^2 I_{1D}(s) \right) \cos(2\pi z s)\, ds \tag{4}$$

where $s = q/2\pi$. It is related to the second derivative of the one-dimensional correlation function

$$g_1(z) = \frac{\partial^2 \gamma_{1D}(z)}{\partial^2 z} + \frac{2K_1}{d_p}\delta(z) \tag{5}$$

where k_1 is the one-dimensional Porod invariant, d_p is the average chord intercept length for the structure, and $\delta(z)$ is a delta function giving the value of the correlation function at the origin. Figure 2 illustrates the relationship between the interface distribution function and structural variables characterizing the contrast density function for a lamellar microphase structure. The polystyrene microdomains have a higher contrast than those of the hydrogenated polybutadiene. The correlation length, L_c, corresponds to the average periodicity between the lamellar microdomains and is obtained from the position of the global minimum in $g_1(z)$. The average thicknesses of the polystyrene and hydrogenated polybutadiene microdomains, d_S and d_{hB}, respectively, are determined from the positions of the local maxima in $g_1(z)$, as indicated in the figure. The interface distribution function has the advantages that the structural information is easily visualized in real-space coordinates and that it is not necessary to model distributions in lamellar thickness and structural disorder.

The direct modeling approach generally requires consideration of the distributions in lamellar thickness and structural disorder. In a perfectly ordered system, the correlation function is periodic in distance. The experimental correlation function however is damped out by disorder factors. Direct consideration of the collective effects of disorder is not possible since there are many types of disorder including lamellar tilt, twist, and thickness variations. The interphases between phases also are not sharp, as depicted in the model contrast density profiles, but narrow diffuse phase boundaries do not appreciably affect the correlation function at large distances[33] and will not be considered herein.

We have found for the purpose of curve fitting that the effects of lamellar disorder on the correlation function can be accounted for empirically by a simple Lorentzian damping function, $P(z)$, of the form

$$P(z) = \frac{1}{1 + (z/\sigma)^2} \tag{6}$$

The parameter σ serves as an estimate of the overall degree of order or disorder in the system. Its magnitude is directly related to the degree of ordering of the lamella. That is, large values indicate less damping of the correlation function and larger areas of structural coherence.

The model approach consists of comparison of the experimental correlation function with a damped theoretical correlation function defined as

$$\gamma^*_{1D}(z) \equiv \gamma_{1D}(z)P(z) \tag{7}$$

where the function $\gamma_{1D}(z)$ is calculated through (1). In applying the model correlation function method, correlation functions are calculated through (7) for model contrast density profiles with a range of styrene microdomain thicknesses and disorder parameters, keeping the interlamellar repeat distance constant. The interlamellar repeat distance was taken as the position of the first maximum in the one-dimensional correlation function. The best fit is determined by the minimum least squared residual error between the experimental (3) and theoretical (7) correlation functions. For simplicities sake, all correlation functions are normalized to a value of unity at the origin.

Solubility limits of the homopolymers within the microdomain structure can be estimated in several ways. In principle, the solubility can be directly calculated from the morphological analysis afforded by the correlation function analysis. A quantitative estimate by this route however requires knowledge of the densities of the microphases.

A relative measure of the homopolymer solubility limits can be realized through calculation of the invariant, Q, defined as

$$Q \equiv \int_0^\infty I(q) q^2\, dq \tag{8}$$

In the case of a two-microphase block copolymer/homopolymer blend containing an overall volume fraction ϕ_m, of microphase separated material, the invariant is given by

$$Q = 2\pi^2 \phi_m \phi_1 \phi_2 (\beta_1 - \beta_2)^2 \tag{9}$$

where the ϕ_i are the relative volume fractions of each microphase. For the neat block copolymer, ϕ_m is unity, and the microphases 1 and 2 refer to the pure components of the copolymer. In the case of a blend, the invariant will decrease if the homopolymers macroscopically demix. The relative magnitude of Q thus reflects the overall degree of which the homopolymer is soluble within the microdomain structure.

Results

Dynamic Mechanical Properties. The mechanical spectra for the block copolymer and blends of the block copolymer with 20 wt % (% bwt) of hB-10, hB-30, hB-60, and hB-120 are shown in Figure 3. At low temperatures, the modulus is constant at $\sim 2 \times 10^9$ Pa for all of the blends. The modulus–temperature curves begin to fall off at −20 °C coincident with the onset of the glass transition of the midblock (T_g = −10 °C). Following this transition is the rubbery plateau region typical of elastomeric block copolymers. Significant differences in

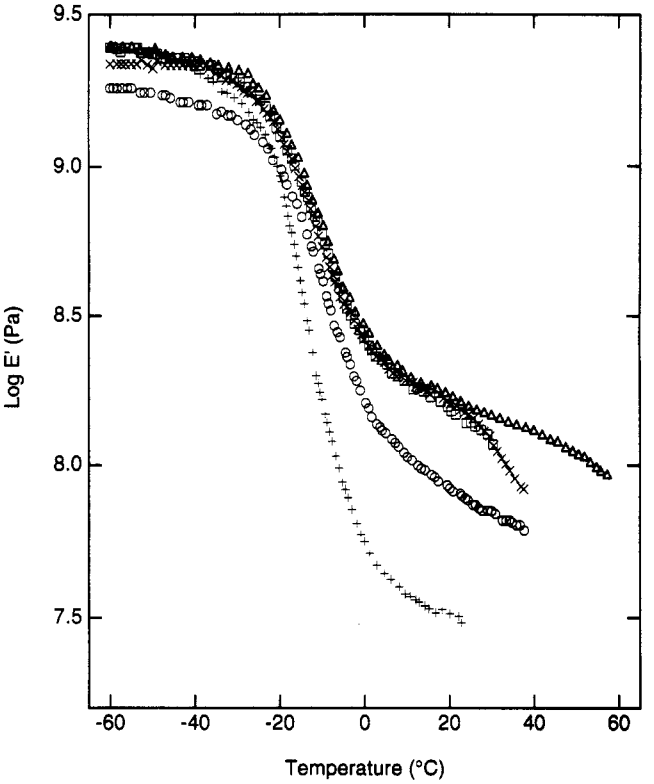

Figure 3. Isochronal plots of E' at 1 rad/s as a function of temperature for hCP (squares), 20% bwt hB-10 blend (plus signs), 20% bwt hB-30 blend (circles), 20% bwt hB-60 blend (triangles), and 20% bwt hB-120 blend (crosses).

behavior are seen for the blends in this region. The plateau moduli for blends containing hB-10 and hB-30 fall below that of the neat copolymer. The mechanical response of the blends with either hB-60 or hB-120 is essentially identical to that of the neat triblock, although the plateau extends to a higher temperature for the hB-60 blend. This behavior is quite remarkable, considering that the content of the glassy, stiff material in the blends is 20% bwt lower than that in the neat copolymer.

This trend can be further illustrated by plotting the storage moduli of these blends at 25 °C and 1 Hz (hereafter designated as the RT modulus) as a function of homopolymer molecular weight. As the homopolymer molecular weight in the blend is increased to that of the midblock (i.e., 60K), the RT modulus (Figure 4) increases to that of the neat block copolymer. The RT moduli of the 20% bwt blends and neat copolymer become equivalent when the homopolymer molecular weight either matches or exceeds the molecular weight of the copolymer midblock with which it associates.

This behavior is contradictory to the predictions of continuum composite theories,[33] since the addition of a rubber to a glass generally diminishes the stiffness. Indeed, an increase in rubber content of neat block copolymers is known to lower the plateau modulus.[39] Addition of hB-X, a rubbery homopolymer to a glassy-rubbery S-hB-S triblock copolymer would therefore be expected to yield a similar decrease in plateau modulus. Models such as that of Takayanagi[40] also predict the opposite of what is observed because the overall fraction of glassy component in the blend is reduced compared to that of the neat copolymer.

Data for the dependence of the RT modulus on both concentration and homopolymer molecular weight are even more remarkable. The data, as shown in Table 2, exhibit an unexpected feature; the addition of a small amount of

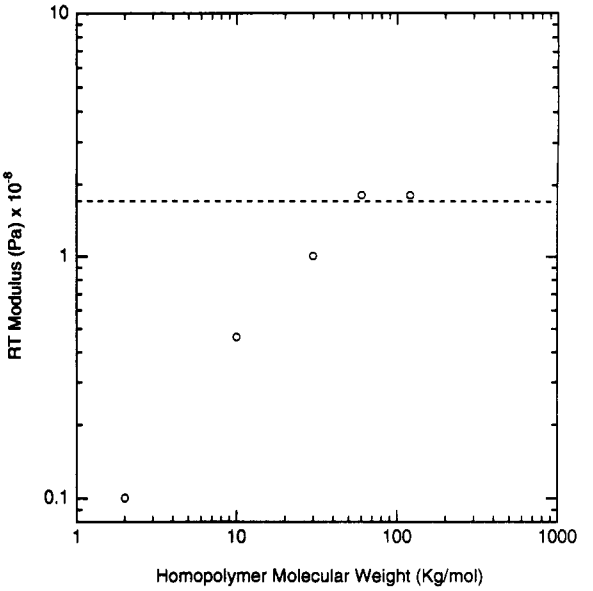

Figure 4. Room temperature modulus (RT) as a function of homopolymer molecular weight. The dashed line denotes the corresponding value for the neat block copolymer.

Table 2. Effect of Homopolymer Concentration on the Storage Modulus $10^{-6}G'$ (Pa) at 25 °C and 1 rad/s

	homopolymer mol wt			
concn wt %	10 K	30 K	60 K	120 K
0	1.70	1.70	1.70	1.70
2.5				2.40
5	1.30			
10	1.40		1.80	2.00
20	0.46	1.00	1.80	1.80

hB-X homopolymer of molecular weight greater than or equal to that of the midblock copolymer leads to an increase in the plateau modulus. This is particularly striking for the blend with hB-120 which shows an increase of over 40% when only 2.5% bwt homopolymer is added. Blends with a homopolymer of molecular weight less than that of the midblock show the expected effect of decreasing the RT modulus due to plasticization. The remainder of this paper is devoted to characterization of the morphology of these blends in an attempt to provide an explanation for these interesting dynamic mechanical properties.

Morphological Characterization. TEM. The micro- and macrophase morphologies of the neat block copolymer and blends can be qualitatively characterized by optical and transmission electron microscopy (TEM) analyses. Figure 5 shows the electron photomicrograph of the neat block copolymer. The bright regions correspond to hB material which is electron-poor compared to the dark polystyrene regions. The microphase structure in this material is clearly lamellar in nature. The addition of small amounts of homopolymer does not significantly alter the microphase geometry observed in the neat copolymer. The predominant morphology remains lamellar for all blends examined. A transition to a cylindrical morphology with polystyrene cylinders might be expected upon homopolymer addition due to the elevated hydrogenated butadiene content. The work of Winey et al.[23] demonstrated that addition of a homopolymer to a symmetric diblock copolymer with lamellar morphology resulted in a transition to a cylindrical morphology. Such a transition is apparently inhibited in our case either as a result of the constraints on both ends of the midblock sequence or due to the use of a casting solvent which is slightly preferential for polystyrene.

Figure 5. Electron photomicrograph of the neat triblock copolymer.

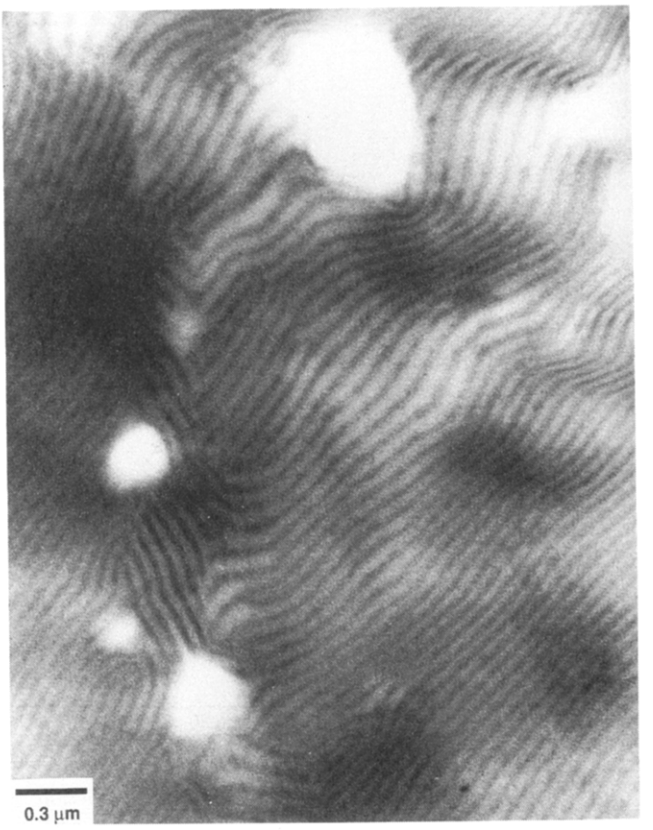

Figure 6. Electron photomicrograph of a 40% bwt blend with hB-60.

Blends with low molecular weight homopolymer do not exhibit any detectable macrophases, indicating that the homopolymer dissolves completely within the midblock microdomains. Blends with higher molecular weight homopolymers show a critical concentration, above which macrophases rich in homopolymer are observed. A typical example of this morphology is seen in Figure 6 for a 40% bwt hB-60 blend. Large, irregular shaped regions rich in homopolymer are observed within a matrix of lamellar microphase structure.

The lamellar microdomains follow the contours of the macrophases, allowing the midblock to contact the chemically identical macrophase as required to minimize the interfacial tension between the matrix and the macrophase. The macrophases are not homogeneously distributed through the lamellar matrix, and they are not always observable within each particular TEM field of view, but their presence can easily be confirmed by examining optical photomicrographs of the same samples.

The macroscopic characterization of blend morphology provides two important conclusions: the geometry of the matrix microphase remains in all cases lamellar, and above a critical concentration, added homopolymer segregates into micron-sized macrophases. Below this critical composition, the homopolymer "dissolves" within a lamellar microphases of the block copolymer.

SANS. The invariant calculations are model independent and reflect qualitatively the solubility limits of the hydrogenated butadiene homopolymers within the midblock lamellae. A more appropriate estimate of the fraction ϕ_m, of microphase separated material can be obtained by properly normalizing the invariant data according to (8). The effect of the volume fraction changes of the microdomains (i.e., $\phi_m \propto Q/\phi_1\phi_2$) is taken into account by dividing all the invariants by the two volume fractions. The value of the ratio of the invariant to the product of the volume fractions therefore serves as a kind of apparent solubility index. The values of ϕ_1 and ϕ_2 required for the normalization are determined by the modeling that follows. This normalization assumes that the contrast density difference of the two microdomains are identical for all of the materials and provides a qualitative estimate of the homopolymer solubility. A more quantitative estimate of ϕ_m requires knowledge of the compositions and densities of the two microphases. For the blends containing 20% bwt homopolymer, the solubility index (Figure 7) falls off rapidly with increasing homopolymer molecular weight. This trend is expected since the combinatorial entropy favoring mixing decreases with molecular weight. It is also consistent with the TEM analysis which showed that macrophases were more apparent in blends containing the higher molecular weight homopolymers.

Our structural analysis consists of modeling the spatial correlation function and determining the interface distribution function by assuming a lamellar system as described earlier. The starting point of the correlation function modeling is to assume that the density fluctuation profile takes the form of a perfectly periodic square wave with the magnitude of the maximum and minimum fluctuations given by the pure component values (e.g. see Figure 1a). These are reasonable assumptions supported by the TEM micrographs (Figures 5 and 6) that show a lamellar structure with relatively sharp microphase boundaries. The ideal correlation function is calculated by numerically autoconvoluting the model contrast density fluctuation profile.

The TEM photomicrographs also show that the spatial coherence of the lamellar structures is limited. This long-range disorder is taken into account by applying the empirical Lorentzian damping function, (6), discussed in the SANS analysis section. In all cases, the model

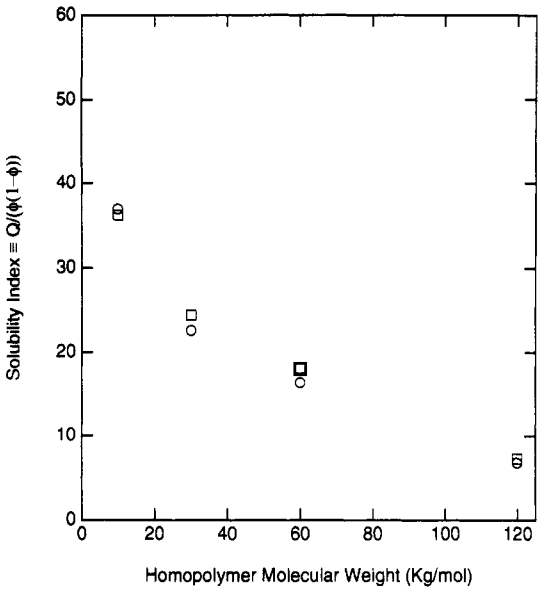

Figure 7. Ratio of the invariant to the product of volume fractions (solubility index) for blends containing 20% bwt homopolymer: from the correlation function analysis (circles) and from the interface distribution function analysis (squares).

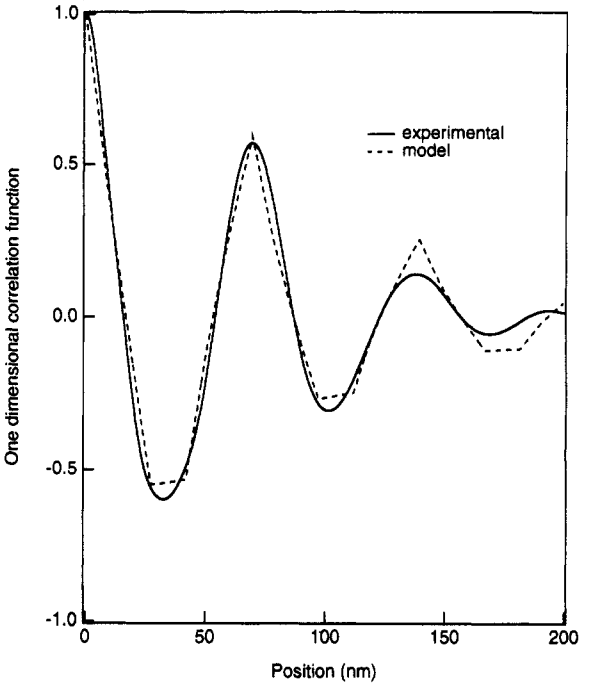

Figure 8. Comparison of the experimental (solid line) and model (dashed line) correlation functions for the neat triblock copolymer.

correlation functions generated in this fashion gave good representations of the experimental correlation functions. A typical comparison of experimental and model correlation functions is shown in Figure 8, for the neat copolymer.

The interface distribution function is obtained directly from the experimental data and assumes only a lamellar geometry for the inhomogeneities. The experimental interface distribution function for the neat copolymer is shown in Figure 9. Although the maxima in the interface distribution are not completely separated, the degree of overlap does not seriously affect the estimation of microphase dimensions from the positions of these maxima. For eample, we have fit the interface distribution function to a series of overlapping Gaussian distribution functions, in order to take into account the possible effects of overlapping distributions. These results, indicated within

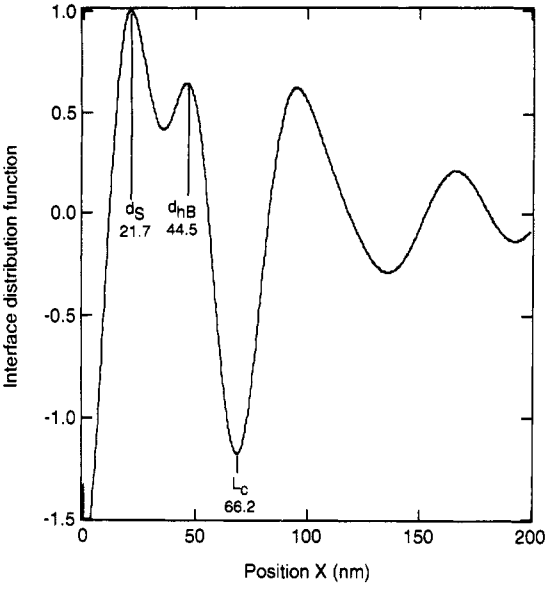

Figure 9. Experimental interface distribution function for the neat triblock copolymer.

Table 3. Results of Model Correlation Function Analysis for 20 wt % Blends

material	L_c (nm)	d_S (nm)	d_{hB} (nm)	ϕ_{hB}	σ
HCP	69.8	27.6	42.2	0.605	1126
HCP/hB-10	65.7	29.9	35.8	0.545	458
HCP/hB-30	69.8	26.8	43.0	0.616	840
HCP/hB-60	76.2	28.1	48.1	0.631	777
HCP/hB-120	68.9	26.9	42.0	0.610	674

Table 4. Results of Interface Distribution Function Analysis for 20 wt % Blends

material	L_c (nm)	d_S (nm)	d_{hB} (nm)	ϕ_{hB}
HCP	66.2 (68.2)	21.7 (22.6)	44.5 (45.6)	0.672 (0.669)
HCP/hB-10	58.8 (58.6)	26.5 (26.5)	32.3 (32.0)	0.549 (0.546)
HCP/hB-30	68.5 (63.0)	22.1 (22.3)	46.4 (40.7)	0.677 (0.646)
HCP/hB-60	72.2 (72.3)	22.2 (22.9)	50.0 (49.4)	0.693 (0.684)
HCP/hB-120	65.5 (61.6)	21.2 (21.5)	44.3 (40.0)	0.676 (0.651)

the parentheses in Table 4, do not differ substantially from the original results neglecting this effect.

The correlation function analysis and the interface distribution function analysis provide independent means for estimating the microphase thickness, the volume fractions of the microdomains, and the interdomain spacings. In addition, the correlation function analysis yields an empirical parameter reflecting the degree of spatial disorder of the lamellae. The trends in the parameters obtained through the two approaches are generally in good agreement, although the absolute values may differ by as much as about 10%. These values are reported in Table 3 for the correlation function analysis and Table 4 for the interface distribution function analysis. The values of interdomain and microdomain thicknesses estimated by the two methods are within 6 nm for all cases.

The degree of spatial coherence of the lamelle can be examined through the disorder parameter, σ, furnished by the correlation function analysis. Larger values of this parameter indicate higher degrees of spatial coherence in the lamellae. The data (Table 3) show that, in all cases, the effect of homopolymer dissolution within the midblock is to disorder the lamellar structure compared to that of the neat copolymer. The degree of disorder is largest for the hB-10 blend, which has the highest apparent homopolymer solubility, but is also significant in the blend with hB-120, where the solubility is lowest.

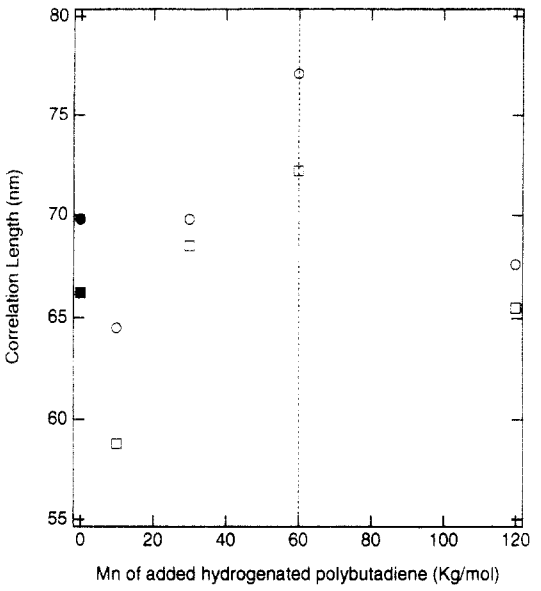

Figure 10. Correlation lengths for blends with 20% bwt of homopolymer as a function of the homopolymer molecular weight. The dashed line represents the molecular weight of the copolymer midblock. The filled symbols denote values for the neat triblock copolymer, the circles are calculated from the interface distribution function analysis, and the squares are determined from analysis of the correlation function.

Experimental correlation lengths for blends containing 20% bwt of hB-*X* are shown in Figure 10, as a function of the homopolymer molecular weight. The vertical dashed line indicates the molecular weight of the hB midblock. The molecular weight behavior is complex, showing microdomain contraction for the lowest molecular weight homopolymer, microdomain swelling for intermediate molecular weight homopolymers, and little change for the highest molecular weight compared to the neat copolymer.

The structural data for the hB-120 blend suggest that most of the homopolymer does not dissolve into the microdomain structure. The low apparent solubility index for this blend (Figure 7) provides additional support for this conclusion. Literature data on diblock copolymer/homopolymer blends show similar behaviors for blends where the homopolymer molecular weight exceeds that of the corresponding copolymer sequence.[41] A low solubility for high molecular weight homopolymers is also to be expected due to the constraints upon the midblock conformation and the relative size of the homopolymer and midblock. The dimension of the midblock microdomain calculated from the scattering analyses falls in the range of 42–45 nm for the neat copolymer. The measured radius of gyration for hB-120 in the melt state is 11.3 nm, approximately equal to the measured radius of gyration of the copolymer midblock sequences (averaged over all lamellar orientations).[13] The hB-120 homopolymer must therefore adopt perturbed configurations in order to reside within the midblock microdomain.

The mechanical property data suggest that the solubility of hB-120 is finite, as the modulus of the 2.5% blend is elevated compared to that of the neat copolymer. A commensurate change in the microdomain dimension accompanying this small solubility would not be detectable with our present experiments. It is possible that these large homopolymer chains become trapped in the midblock microdomain during the solution casting process and do not reflect any equilibrium structure. It is interesting to note however that these systems with extremely low homopolymer solubility show the largest increases in plateau modulus.

The microdomain structure swells for blends with hB-60 as a result of increased homopolymer solubility (see Figure 7). The radius of gyration of this homopolymer (7.7 nm[13]) is small enough that it can be accommodated within the midblock microdomain. The observed degree of swelling is consistent with what has been found previously for diblock copolymer/homopolymer blends.[42]

Interesting behavior is seen for the blends containing the two lowest molecular weight homopolymers. Although the apparent homopolymer solubility is greater than for the higher molecular weight blends, the correlation length is smaller than that of the hB-60 blend. The question then is how the microdomains can shrink when more homopolymer is added to them?

One possible explanation for microdomain shrinkage upon homopolymer addition is furnished by consideration of the constraints imposed upon the midblock microdomain of the neat block copolymer. In a neat block copolymer system with lamellar microdomains, the copolymer sequences must stretch in order to fill space in the center of the microdomain. Experimental SANS results for diblock copolymers have demonstrated that the copolymer sequences are extended perpendicular to the lamellae and contracted in-plane with respect to unperturbed dimensions.[43–45] Neutron scattering experiments on our block copolymer system confirm that the midblock chains are stretched.[13] The radius of gyration (averaged over all orientations) is 11.4 nm compared to the expected values of 9.9 nm for an unperturbed homopolymer of the same apparent molecular weight as the midblock sequence. The dimensions of the midblock microdomains and the interdomain repeat distance of the copolymer reflect this stretching. For example the correlation length for block copolymers is known to scale approximately with the two-thirds power of molecular weight,[46] compared to unperturbed chains, whose radius of gyration scales with the one-half power of molecular weight.

It is possible for the microdomain to shrink if the homopolymer reduces these constraints on the midblock. For high molecular weight homopolymers it is virtually impossible for the chain to configure itself in a fashion which would relieve these constraints. Low molecular weight additives, however, can relieve these constraints by distributing preferentially in the center of the midblock microdomain. In this scenario, the stretching of the midblock sequence could relax, causing a decrease in microdomain thickness, and an expansion of the microdomain in the in-plane direction. The latter expansion would not be detected by scattering experiments. Microdomain contraction of this nature has been seen experimentally in diblock copolymer blends,[42] and homopolymer localization of this nature has been proposed for block copolymer blends.[33,47,48] SANS experiments on specially labeled block copolymers, presented in a related paper,[25] confirm that some of the low molecular weight homopolymer is preferentially localized in the center of the midblock.

The volume fractions determined through scattering analysis are shown in Figure 11. The data for the hB microphases reflect the trends observed in the correlation function. The hB microdomains appear to shrink for the blend with lowest molecular weight homopolymer (see also the microdomain thickness data in Tables 3 and 4), progressively expand for blends with homopolymers of molecular weights similar to that of the midblock, and then return to the value of the neat block copolymer for

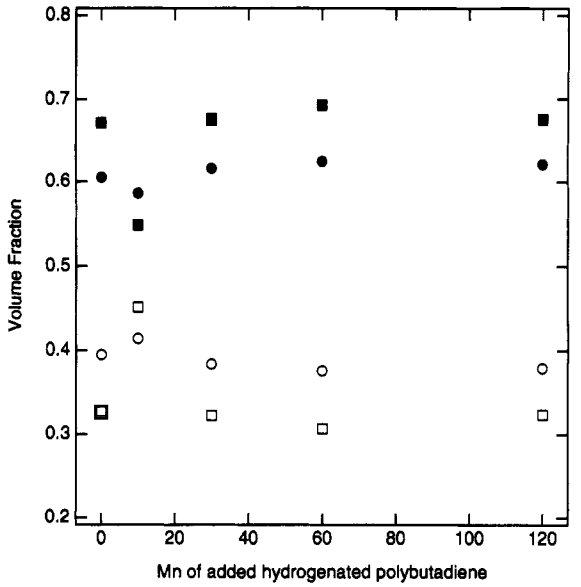

Figure 11. Estimated microphase volume fractions for 20% bwt blends. Values determined by the model correlation function analysis are for polystyrene (open circles) and for hydrogenated polybutadiene (filled circles). Values obtained by correlation function modeling are for polystyrene (open squares) and for hydrogenated polybutadiene (filled squares). Volume fractions for the neat triblock copolymer are displayed as a value of $M_n = 0$.

high molecular weight homopolymers with negligible solubility.

The shrinkage of the hB microdomains for the hB-10 blend appears to be accompanied by an expansion of the polystyrene microdomains (Tables 3 and 4). The swelling of the midblock microdomains in the hB-60 blend, on the other hand, does not alter the average thickness of the polystyrene microdomains. The observed trends are in conflict with general expectations regarding the interfacial area per block copolymer chain junction, which must be the same on both sides of the interphase. In general, chain swelling due to preferential homopolymer solubility on one side of the interphase must be accompanied by chain contraction on the other side.[42] This would not be required, however, if the interphase curvature changes or if the homopolymer is not homogeneously distributed within the midblock microdomain, as discussed earlier.

Comparison of the SANS data on microdomain thicknesses and volume fractions with expected values for these parameters calculated from the known blend compositions can in principle be used to calculate quantitative homopolymer solubility limits for the blends. Unfortunately, the cumulative errors within this calculation appear to be too large to permit quantitative assessments. For example, the correlation function and interface distribution function methods provide independent means for characterizing the microphase structure. An estimate in the accuracy in determination of the structural parameters can therefore be obtained by comparison of the results from the two distinct approaches. While results from the two approaches show qualitatively similar trends, they differ quantitatively by as much as 0.07 in the respective volume fractions, indicating a large error in the determination of these quantities. The reason for these differences lies in the different manner in which the two methods take into account the distributions of microdomain thickness, as well as errors in regression of the models. The large deviation between the two data sets may suggest either that these distributions are very broad or that the simple one-dimensional models employed are not completely appropriate in describing the blend morphologies. Calculations of the theoretical volume fraction of the hydrogenated polybutadiene phase predict a value of 0.66, if all of the homopolymer dissolves, and 0.565 if none of the homopolymer dissolves. The error in the volume fractions determined from the scattering analysis is of the same order of magnitude as the anticipated change in volume fraction expected due to solubility differences, and thus the calculation of solubility limits is not possible.

The qualitative trends in these data also appear to be inconsistent with what is anticipated. From the invariant analysis and entropic considerations, the lowest molecular weight homopolymer is expected to have the highest solubility and consequently the highest hydrogenated polybutadiene volume fraction. We find just the opposite behavior for the hB-10 blend. This is at least partially a result of the heterogeneity of structure in this blend. While the SANS results in the present paper show only one scattering maximum corresponding to a contracted lamellar structure, SANS studies on a similar isotopically labeled hB-10 blend[25] suggest that there exist two distinct morphologies for this blend: one contracted and one expanded. Due to the manner in which scattering techniques weight various contributions, the expanded structure is seen only in the SANS data and is not observable by X-ray scattering on the same sample. In other words, if two distinct morphologies exist in any of the blends, the simple one-dimensional models employed herein cannot adequately describe their overall morphology. While we know this to be true for the hB-10 blend, there is not sufficient SANS contrast in the other blends, due to the low homopolymer solubility, to examine this possibility.

Another possible complication in these analyses is the possibility of partial phase mixing. As the molecular weight of the homopolymer is decreased, the microphase structure itself becomes less stable, until, eventually, a molecular weight is reached at which a single disordered phase is obtained.[22] As this order–disorder transition is approached, the compositions of the coexisting microphases must become progressively closer to each other, similar to the behavior seen in Figure 11, as the hB homopolymer molecular weight is decreased. DSC analysis of the blend T_g's,[33] however, shows that they are virtually unchanged from that of the neat copolymer, providing evidence against the existence of significant microphase mixing.

Summary Discussion

The results of mechanical testing demonstrate that the addition of rubbery homopolymers to the elastomer midblock of a triblock copolymer causes unusual changes in the plateau modulus. For low molecular weight homopolymers, the modulus decreases with the homopolymer content, as would be expected. For homopolymers with molecular weight equal to that of the midblock sequence, the modulus is constant for low homopolymer content and eventually decreases at high contents. For homopolymers with molecular weight exceeding that of the midblock sequence, the plateau modulus increases when a small amount of homopolymer is added and then decreases with further addition beyond a critical composition.

The gross morphology of the microdomains remains lamellar for all blends studied. There is observed, however, a critical concentration of homopolymer above which macrophases consisting of undissolved homopolymer are found. The apparent homopolymer solubility decreases

rapidly with homopolymer molecular weight and is very low for the highest molecular weight homopolymer blend.

A thorough analysis of the microdomain structure through SANS analysis provides equally unusual results. The structure of the highest molecular weight blend is essentially identical to that of the neat copolymer, reflecting the limited solubility of the homopolymer within the midblock microdomain. Blends with intermediate molecular weight homopolymers (i.e., equal to or slightly less than the molecular weight of the midblock) exhibit swelling of the midblock microdomains due to the increased solubility of the homopolymers. The blend containing the homopolymer of lowest molecular weight but of highest relative solubility gives the unusual result that the midblock microdomain shrinks upon homopolymer addition.

Our goal is to provide a reasonable explanation for the unusual mechanical property behavior of these copolymer blends based upon the morphological information provided by our detailed structure analysis. The complicated nature of these materials and the unusual results obtained make this task difficult; however we would like to offer the following initial explanations for our results.

The behavior of the hB-10 blends can be understood by considering the packing constraints for a lamellar block copolymer. It is difficult for Gaussian chains to form densely packed lamellae since they are more or less spherical and would leave density defects in the center of the microdomain. Block copolymer chains must therefore stretch out to fill space in the microdomain center by adopting extended configurations. Previous SANS experiments have demonstrated that diblock copolymer sequences are extended normal to the lamellae and that they are contracted parallel to the lamellar plane.[43-45] Extended conformations for the midblock chains in the hCP triblock copolymer have been confirmed by our own SANS experiments.[13]

The extended perturbed configuration adopted by the midblock sequences in the neat copolymer are represented schematically in Figure 12a. Midblock sequences in both the loop and traversing configurations adopt extended configurations, as indicated by the cross-hatched ellipses. The space filling constraint responsible for the chain extension can be relaxed if the homopolymers localize preferentially at the center of the midblock microdomain, as depicted schematically in Figure 12b. The results of SANS experiments[25] confirm that at least some of the homopolymer chains localize in this fashion. In addition, localization of this nature has been proposed to occur for block copolymer blends,[47,48] and has been observed experimentally for other block copolymer blend systems.[42,49]

As the homopolymer chains fill space at the center of the microdomain, the block copolymer chains can relax to a less extended, more spherical distribution. The microdomain can thus shrink in the direction normal to the lamellae but expand in the in-plane direction. The details of this picture are difficult to establish, since there exist two basic configurations for the midblock sequence: a tie chain penetrating from one side to the other of the lamellae or a loop which leaves and returns from the same side of the lamellae. The fraction of each of these conformations has not yet been determined for any triblock copolymer. The existence of these two conformations could lead to lateral concentration fluctuations in the homopolymer concentration if the conformations were not randomly distributed. The increase in lamellar disorder observed for the blends (see σ values in Table 3) is consistent with

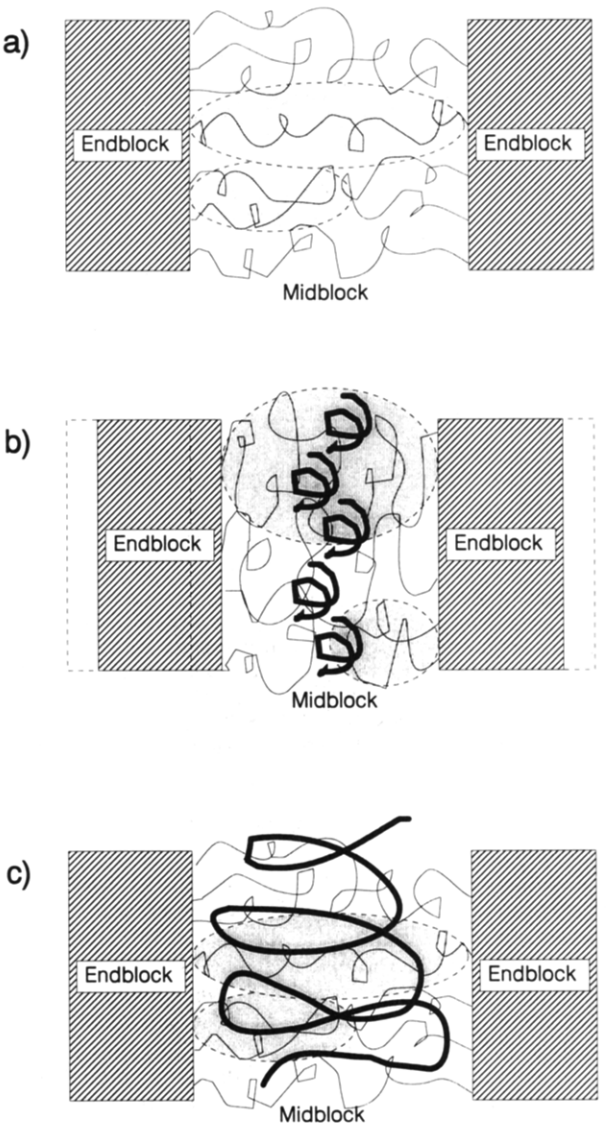

Figure 12. Schematic diagrams illustrating possible molecular structures for the midblock microdomains in (a) the neat triblock copolymer, (b) the 20% bwt blend with hB-10, and (c) the 20% bwt blend with hB-120. The cross-hatched ellipses indicate the approximate spatial distributions of the midblock chains, where the smaller ellipses refer to chains in the loop configuration and the larger ellipses are associated with configurations which traverse the lamellar. The homopolymer chains are indicated by the thicker lines.

this kind of heterogeneity, and the SANS results on isotopically labeled materials[25] suggest that a second, expanded structure is also present in this blend. The simple one-dimensional models employed in the present study thus are not completely adequate in describing the morphology of these rather heterogeneous systems.

The mechanical response of the blends with hB-10 can be explained through this schematic structure. The addition of a low molecular weight homopolymer dilutes the number of chain entanglements and would decrease the apparent plateau modulus regardless of the homopolymer distribution. In addition, the increased overall content of rubbery component in the blend also contributes to a diminishment of the plateau modulus.

The blend with hB-30 exhibits intermediate behavior. The microdomain dimensions are almost unchanged from those of the neat copolymer, even though a substantial fraction of the homopolymer dissolves within the microdomain structure. It is more difficult for this molecular

weight homopolymer to localize at the microdomain center due to its larger size. There appears to be a balance point at this molecular weight where the swelling due to the increased rubber content is compensated for by contraction due to localization of some of the homopolymer at the microdomain center. The plateau modulus falls upon addition of this homopolymer since, being of lower molecular weight than the midblock, it again dilutes the entanglements. The magnitude of the modulus decrease is smaller than that of the hB-10 blends since hB-30 is more highly entangled than hB-10.

The microdomains in the hB-60 blend are swollen, since the size of the midblock and homopolymer are similar. The homopolymer can no longer easily configure itself into the microdomain, and the solubility decreases compared to that of the lower molecular weight blends. It is not clear how the swelling occurs, since some of the midblock sequences form tie chains that might limit swelling. It is possible that the swelling is inhomogeneous, occurring primarily at positions within the lamellae where there is a predominance of loop configurations. Where there are loop configurations, the midblock chains form a bilayer structure. The homopolymer can simply split the bilayer and locate between the two resultant loop layers. SANS analyses[25] of deuterium labeled systems support the presence of this type of structure in the hB-10 blend.

The plateau moduli of the hB-60 blends (see Table 2) are approximately equal to that of the neat copolymer, contrary to what is expected when the rubbery content of an elastomer is increased. Addition of 20% bwt of a rubber to an elastomer would be expected to decrease the modulus by a corresponding amount. In our case we actually observe an almost constant modulus, most probably associated with changes in the entanglement structure of the midblock. As was pointed out earlier, block copolymer chains have been shown to present configurations that are extended normal to the lamellar plane and contracted within the lamellar plane. The degree of lateral intermolecular interpenetration is necessarily lower in these perturbed conformations than in the unperturbed state due to the lateral contraction, and therefore the number of entanglements (and the plateau modulus) must decrease. The larger than expected plateau modulus obtained upon homopolymer addition can be understood if it leads to an increase in the number of entanglements in the midblock microdomain. This improvement in entanglement structure apparently compensates for the effect of an increase in the rubber content, to lead to a plateau modulus that is essentially unchanged from that of the neat copolymer.

This mechanism is perhaps clearer for the blends with hB-120. The microdomain dimensions of these blends are essentially unchanged; however there is a small but finite solubility of the homopolymer within the midblock. The hB-120 homopolymer chain is larger than the midblock chains and therefore cannot orient in the direction normal to the lamellae as do the midblock chains. In fact, it most probably must orient in the direction parallel to the lamellae (i.e., normal to the midblock chains) in order to fit in the confined space offered by the lamellae. This process serves to effectively weave together the homopolymer and midblock chains with the midblocks serving as a warp and the homopolymers playing the role of the weft.

A schematic representation of a hypothetical structure for the 20% bwt hB-120 blend is drawn in Figure 12c. The midblock chains are expected to be extended normal to the lamellae and contracted in the in-plane directions, as indicated by the cross-hatched ellipses. The contraction leads to poor lateral interpenetration of the chains and consequently a poor lateral entanglement network. Addition of the homopolymer effectively weaves a network of laterial entanglements in the system, causing an increase in the plateau modulus. Since the molecular weight of the homopolymer is high, only a small number of homopolymers need reside within the midblock in order to increase drastically the number of entanglements.

This scenario provides an explanation for the fact that the addition of only 2.5% bwt of hB-120 leads to an increase of almost 50% in the plateau modulus. The addition of further amounts of homopolymer leads to a decrease in the modulus. This latter trend is consistent with our observation of a critical solubility concentration. It seems reasonable to associate the concentration at which the maximum modulus is observed with the critical solubility limit. Addition of homopolymer beyond this limit simply leads to macrophase separation of the insoluble rubber, which necessarily decreases the modulus. From our mechanical property data one might then conclude that the solubility limit of hB-120 is about 2.5% bwt. This small magnitude is consistent with our finding that the microdomain dimensions for these blends are not substantially different from those of the neat copolymer.

Although the interpretations presented above are still speculative, our results clearly demonstrate that interesting and unusual properties can be obtained by blending triblock copolymers with homopolymers. This interesting behavior differs markedly from that of diblock copolymer blends and is most likely associated with the effects of the strong constraints enforced upon chains in confined geometries such as a copolymer midblock. There appears to be strong heterogeneity in the local structure in blends of this nature, perhaps due to the possibility of both looplike and tie-chain configurations for the midblock sequences. Results from scattering analysis based upon simple one-dimensional lamellar models are therefore found to be, in some cases, inconsistent with the expectations of simple additivity, ruling out any possibility of making quantitative structure–property correlations based upon the present data. Many questions remain to be answered for these systems, and further experimentation must be performed in order to validate our hypotheses.

Acknowledgment. The authors wish to acknowledge financial support provided by the Cottrell Research Program of the Research Corp., and the Petroleum Research Fund, administered by the American Chemical Society. The work at ORNL was sponsored in part by NSF Grant No. DMR-7724459 through Interagency Agreement No. 40-636-77 with the U.S. Department of Energy under Contract No. DE-AC05-840R21400 to Martin Marietta Energy Systems, Inc. J.P.B. wishes to acknowledge support through grants from The Shell Development Co. and the University of Connecticut Research Foundation. Most of the experimental work reported in this paper was performed while X.Q., I.G., and J.T.K. were associated with Princeton University.

References and Notes

(1) Present address: Technical University of Wroclaw, Wroclaw, Poland.
(2) Present address: AT&T Bell Laboratories, Murray Hill, NJ 07974.
(3) To whom correspondence should be addressed.
(4) Molau, G. E. In *Colloidal and Morphological Behavior of Block and Graft Copolymers*; Aggarwal, S. L., Ed.; Plenum: New York, 1970.
(5) Anastasiadis, S. H.; Gancarz, I.; Koberstein, J. T. *Macromolecules* **1989**, *22*, 1449.

(6) Kraus, G. In *Block Copolymers: Science and Technology*; Meier, D. J., Ed.; MMI, Gordon & Breach Science Publishers: London, 1983.
(7) Kraus, G.; Rollmann, K. W.; Gruver, J. T. *Macromolecules* **1970**, *3*, 92.
(8) Kotaka, T.; Miki, T.; Arai, K. *J. Macromol. Sci.—Phys.* **1980**, *B17* (2), 303.
(9) Riess, G.; Schlienger, M.; Marti, S. *J. Macromol. Sci.—Phys.* **1980**, *B17* (2), 355.
(10) Kim, J.; Han, C. D.; Chu, S. G. *J. Polym. Sci., Polym. Phys. Ed.* **1988**, *26*, 667.
(11) Owens, J. N.; Gancarz, I.; Koberstein, J. T.; Russell, T. P. *Macromolecules*, **1989**, *22*, 3380.
(12) Owens, J. N.; Gancarz, I.; Koberstein, J. T.; Russell, T. P. *Macromolecules* **1989**, *22*, 3388.
(13) Quan, X.; Gancarz, I.; Koberstein, J. T.; Wignall, G. D. *J. Polym. Sci., Polym. Phys. Ed.* **1987**, *25*, 641.
(14) Quan, X.; Gancarz, I.; Koberstein, J. T.; Wignall, G. D. *Macromolecules* **1987**, *20*, 1431.
(15) Inoue, T.; Soen, T.; Hashimoto, T.; Kawai, H. In *Block Copolymers*; Aggarwal, S. L., Ed.; Plenum: New York, 1970.
(16) Inoue, T.; Soen, T.; Hashimoto, T.; Kawai, H. *Macromolecules* **1970**, *3*, 87.
(17) Kawai, H.; Inoue, T. *Jpn. Plast.* **1970**, 12.
(18) Aggarwal, S. L.; Livigni, R. A. *Polym. Eng. Sci.* **1970**, *17*, 498.
(19) Skoulios, A.; Helffer, P.; Gallot, Y.; Selb, J. *Die Makromol. Chem.* **1971**, *148*, 305.
(20) Kohler, J.; Riess, G.; Banderet, A. *Eur. Polym. J.* **1968**, *4*, 173.
(21) Roe, R.-J.; Zin, W.-C. *Macromolecules* **1984**, *17*, 189.
(22) Whitmore, M. D.; Noolandi, J. *Macromolecules* **1985**, *18*, 2486.
(23) Winey, K. I.; Thomas, E. L.; Fetters, L. J. *Macromolecules* **1992**, *25*, 2645.
(24) Han, C. D.; Kim, J.; Baek, D. M.; Chu, S. G. *J. Polym. Sci., Polym. Phys. Ed.* **1990**, *28*, 315.
(25) Lee, S. H.; Koberstein, J. T.; Quan, X.; Gancarz, I.; Wignall, G. D.; Wilson, F. C. *Macromolecules* **1994**, *27*, 3199.
(26) Halasa, A. F.; Lohr, D. F.; Hall, J. E. *J. Polym. Sci., Polym. Chem. Ed.* **1981**, *19*, 1357.
(27) Fetters, L. J. *J. Polym. Sci.* **1969**, *C26*, 1.
(28) Falk, J. C. *J. Polym. Sci., Polym. Chem. Ed.* **1971**, *9*, 2617.
(29) Falk, J. C.; Schlott, R. J. *Macromolecules* **1971**, *4*, 152.
(30) Falk, J. C. *Die Makromol. Chem.* **1972**, *160*, 291.
(31) Handlin, D. L.; Thomas, E. L. *Macromolecules* **1983**, *16*, 1514.
(32) Koehler, W. C.; et al. *Scattering Techniques Applied to Supramolecular and Non-Equilibrium Systems*; Chen, S. H., et al., Eds.; NATO Advanced Study Series 83; Plenum: New York, 1980.
(33) Quan, X. S. Ph.D. Dissertation, Princeton University, Princeton, NJ, 1986.
(34) Hosemann, Z. *Phys.* **1949**, *127*, 16.
(35) Vonk, C. G; Kortleve, G. *Kolloid Z. Z. Polym.* **1967**, *220*, 19.
(36) Strobl, G. R.; Schneider, M. *J. Polym. Sci., Polym. Phys. Ed.* **1980**, *19*, 1343.
(37) Kortleve, G.; Vonk, C. G. *Koll. Z. Z. Polym.* **1968**, 124.
(38) Ruland, W. *Colloid Polym. Sci.* **1977**, *255*, 5, 417.
(39) Ferry, J. D. *Viscoelastic Properties of Polymers*; John Wiley & Sons: New York, 1961.
(40) *Block Copolymers*; Allport, D. C., Janes, W. H., Ed.; Halsted, New York, 1973.
(41) Mayes, A. M.; Russell, T. P.; Satija, S. K.; Kajkrzak, C. F. *Macromolecules* **1992**, *25*, 6523.
(42) Winey, K. I.; Thomas, E. L.; Fetters, L. J. *Macromolecules* **1991**, *24*, 6182.
(43) Hadziioannou, G.; Picot, C.; Skoulios, A.; Ionescu, M.-L.; Mathis, A.; Dupplesix, R.; Gallot, Y.; Lingelser, J.-P. *Macromolecules* **1982**, *15*, 263.
(44) Hasegawa, H.; Hashimoto, T.; Kawai, H.; Lodge, T. P.; Amis, E. J.; Glinka, C. J.; Han, C. C. *Macromolecules* **1985**, *18*, 67.
(45) Matsushita, Y.; Mori, Y.; Saguchi, R.; Noda, I.; Nagasawa, M.; Chang, T.; Glinka, C. J.; Han, C. C. *Macromolecules* **1990**, *23*, 4317.
(46) Helfand, E.; Wasserman, Z. In *Developments in Block Copolymers*; Goodman, I., Ed.; Applied Science: Essex, England, 1982; Volume 1.
(47) Hashimoto, T.; Tanaka, H.; Hasegawa, H. *Macromolecules* **1990**, *23*, 4378.
(48) Shull, K. R.; Winey, K. I. *Macromolecules* **1992**, *25*, 2637.
(49) Berney, C. V.; Cheng, P.-L.; Cohen, R. *Macromolecules* **1988**, *21*, 2235.